

ORIGINAL ARTICLE

Modified Dynamic Model for Longitudinal Motion of Ground Vehicles

N. Sina^{1,2}, M.R.H. Yazdi^{1*} and V. Esfahanian^{1,2}¹School of Mechanical Engineering, College of Engineering, University of Tehran, College of Engineering-campus 2, North Kargar ave., P.O. box 11155-4563 Tehran, Iran²Vehicle, Fuel and Environment Research Institute (VFERI), University of Tehran, P.O. box 14395-1335, Tehran, Iran
Phone: +982161119916; Fax: +982188013029

ABSTRACT – The present study aims to provide a modified model for analysing the longitudinal dynamics of ground vehicles. Bearing in mind that an inevitable tire slip occurs under the transmission of driving torque to the drive wheels, the pure rolling assumption employed in many previous works is modified in this research. This paves the way through the development of a more realistic simulation framework with promising performance when used in vehicle and powertrain related topics. The modified equation of motion is an explicit function of tire slip ratio, and as a result, by rewriting the power balance equation, a dissipation term due to tire slip appears, which is consistent with the outcome of the recent contributions. Simulation results indicate a significant difference between the modified and simplified models in the case of a relatively high tractive force. Moreover, tire slip loss is obviously large in such a case, so that its neglect would lead to a noticeable inaccuracy in the response of the traditional model. An average of 35% improvement in the accuracy of prediction of tire consumed energy is observed in 0 to 100 km/h half-throttle acceleration manoeuvre using the modified model.

ARTICLE HISTORYReceived: 16th April 2020Revised: 27th Oct 2020Accepted: 7th Jan 2021**KEYWORDS**

Vehicle dynamics;
Dynamic model;
Longitudinal motion;
Tire slip;
Slip loss

NOMENCLATURE

a_x	longitudinal acceleration, m/s ²	<i>Superscripts</i>	
A	area, m ²	*	characteristic
c_D	drag coefficient, –	<i>Subscripts</i>	
E	energy, J	a	air
f	coefficient, –	c	characteristic
F	force, N	d	drive wheels
g	gravitational acceleration, m/s ²	D	aerodynamic drag
k	tire stiffness, N/m ²	dyn	dynamic
m	mass, kg	e	engine
P	power, W	f	front
q	force distribution, N/m	Gr	road grade
r	radius, m	in	inertia
T	torque, Nm	n	non-drive wheels
v	velocity, m/s	r	rear
η	driveline efficiency, –	rel	relative
λ	slip ratio, –	R	rolling resistance
μ	coefficient of friction, –	S	sliding or slip
θ	road angle, rad	st	static
ρ	density, kg/m ³	t	tire
σ	stress distribution, N/m	w	wheel
ω	angular velocity, rad/sec	x	longitudinal
		z	vertical
EPA	Environmental Protection Agency		
FTP	federal test procedure		
FWD	front-wheel drive		
HIL	hardware in the loop		
IEA	International Energy Agency		
NEDC	new European driving cycle		
SIL	software in the loop		
WLTP	worldwide harmonised light vehicles test procedure		

INTRODUCTION

Longitudinal modelling is the basis of several fields of study in automotive engineering, for instance, energy and fuel consumption, safety systems, and intelligent transportation. In a V-model development process, a more accurate model would diminish the performance degradation in hardware-in-the-loop (HIL) simulation comparing to software-in-the-loop (SIL) simulation, and consequently, design validity would be improved as well as reduction of development cost and time [1]. In the model that has been widely used for the study of vehicle longitudinal motion, it is assumed that the wheel purely rolls with no slip. It is notable that in the forward simulation of longitudinal motion, usually drive wheel(s) is treated as an additional degree of freedom (DOF) in order to observe the longitudinal tire slip, which is then being used to obtain the tractive force by means of an appropriate tire model. However, pure rolling of the wheels is assumed prior to extracting the vehicle's equation of motion [2,3]. This assumption makes the model simpler, though model accuracy decreases as far since tire slip inevitably occurs whenever a driving torque is applied to the wheel [4]. Accordingly, the model provides an inadequate response, which is a drawback, especially when implementing model-based controllers or using identification methods [5,6]. Therefore, defining a modified longitudinal model to rely more on the physics of the situation by considering the tire slip would improve the validity of the model and its compliance with the actual plant.

Investigation of vehicle energy demand and resistant powers is identified as one of the demanding topics in automotive engineering, especially in recent years, owing to the current share of oil consumption in the transport sector. According to International Energy Agency (IEA) reports, more than half of the global oil consumption in 2012 corresponded to the road transport sector [7], a really enormous amount that demonstrates a high potential to reduce CO₂ emission and to approach 2-degree global warming pathway. Accordingly, it could be stated that a thorough analysis of vehicle energy demand and its breakdown is crucial in treating the resistant forces and developing more efficient vehicles. However, in the vehicle models that have been utilised to analyse the energy demand, pure rolling of the wheels is a priori assumed which affects the validity of results. When the pure rolling of the drive wheels is assumed in the modelling, resistance powers are comprised of inertia, aerodynamic drag, road grade, and tire rolling resistance, while a term in power losses that occurs due to tire slip has been omitted. Accordingly, the authors in [8] introduced the modified tire resistance, which includes tire slip resistance as well. Experimental results have shown that tire slip loss should be taken into account in order to accurately observe the influence of tire on the fuel efficiency of ground vehicles [9]. Nevertheless, it has not been investigated in similar studies, e.g. in [10–13], and as a consequence, rolling resistance has been defined as the sole power dissipation in tires.

This paper proposes a modification to the vehicle longitudinal model by considering the tire slip, which to the best of the authors' knowledge, has been neglected in previous researches to obtain the dynamic model. Additionally, current study looks forward to investigate the vehicle energy demand using simplified and modified vehicle models and to show how much difference the modified model can make in different driving conditions. To achieve this, the paper is organised as follows: tire physical model is briefly explained in Section 2. Vehicle longitudinal motion is remodelled by taking the general motion of the drive wheel, including rolling and slip, into account. Then, resistant powers in the modified model are explored in Section 4 and the results of simulation are discussed in Section 5. Finally, some conclusions are drawn in the last section.

TIRE MODEL

When a driving torque applies to the wheel, the wheel centre travelled distance is less than that of a free-rolling wheel [4]. As it is illustrated in Figure 1, in this case, the wheel rolls and slips simultaneously and this phenomenon is known as tire slip. Several equations have been proposed for the tire longitudinal slip ratio. Although some equations are standardised, one of the practical equations is given by Eq. (1).

$$\lambda = \frac{v_s}{r_{dyn}\omega_w} = \frac{r_{dyn}\omega_w - v_x}{r_{dyn}\omega_w} \quad (1)$$

where λ is longitudinal slip ratio, v_s is sliding velocity, ω_w is wheel angular velocity, r_{dyn} is the dynamic radius of the wheel, and v_x is the longitudinal speed that can be expressed as:

$$v_x = r_{dyn}\omega_w - v_s = r_{dyn}\omega_w(1 - \lambda) \quad (2)$$

Effective radius (see Figure 1) is the radius that correlates the angular velocity to longitudinal slip, which could be obtained using Eq. (2) as:

$$r_{eff} = \frac{v_x}{\omega_w} = r_{dyn}(1 - \lambda) \quad (3)$$

Considering the standard equation given by [14,15], the slip ratio varies in an asymmetric range from -100% to infinity, where negative and positive ratios correspond to braking and accelerating conditions, respectively. To define the slip ratio in the same scale for accelerating and braking (between 0 to 100%), a piecewise function has been defined that for acceleration, represented by Eq. (1). Another advantage rising by defining Eq. (1) is that the proposed ratio is also representative of bristle deformation (see Appendix 1).

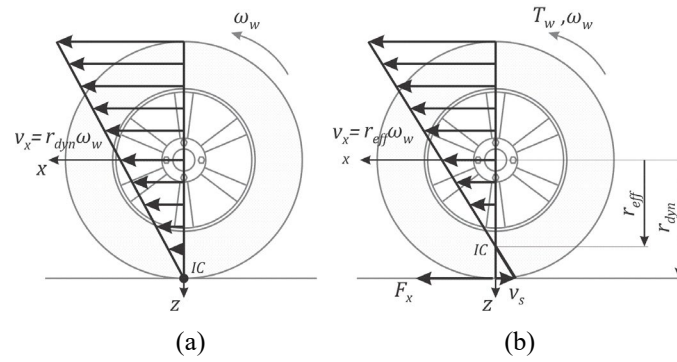


Figure 1. Velocity profile of the wheel at (a) pure rolling and (b) combined rolling and slipping.

Generated force in the contact area between tire and ground is a function of tire slip. The tire physical model (or brush model) provides a framework to interpret tire force from tangible physical parameters, such as coefficient of friction and tire stiffness. This gives the physical model a distinctive advantage over empirical tire models. In the physical model, contact patch is considered to be divided into two regions, namely adhesion and sliding. The interacting force in the adhesion region is determined by the tire elastic properties, while the interacting force in the sliding region depends on tire and ground adhesive properties. A characteristic length, x_c , is defined such that it denotes the boundary of the adhesion and sliding regions. Hence, as it is shown in Figure 2, for the adhesion region $x \leq x_c$ and for the sliding region $x > x_c$. Consequently, the stress distribution can be summarised as [16]:

$$\sigma(x) = \begin{cases} k_x \lambda (a - x) & a > x > x_c \\ \mu_x q_z x_c & x_c > x > -a \end{cases} \tag{5}$$

where k_x is tire longitudinal stiffness and μ_x is the longitudinal coefficient of friction. Also, q_z represents normal force distribution that several forms, e.g. parabolic and trapezoidal, have been proposed for. We assume a parabolic normal force distribution, given by Eq. (6) [17].

$$q_z(x) = \frac{3F_z}{4a} \left(1 - \left(\frac{x}{a} \right)^2 \right) \tag{6}$$

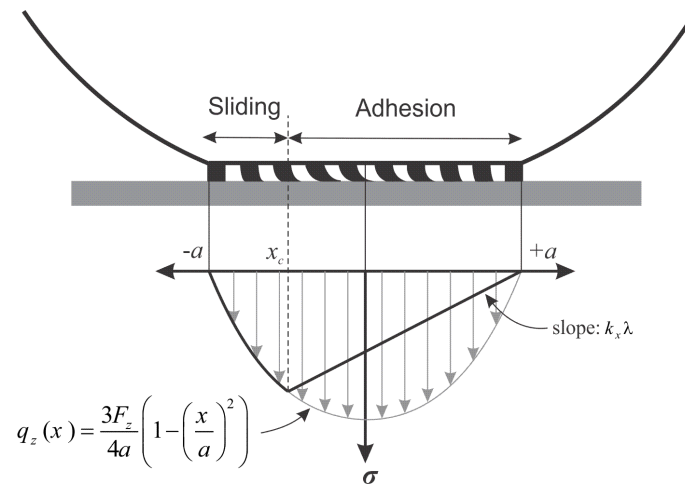


Figure 2. Schematic of tire deformation and stress distribution.

The condition for sliding to occur is that the stress in the adhesion region becomes larger than that of the sliding region. Hence, the sliding condition could be given by:

$$k_x \lambda (a - x) \geq \mu_x q_z \tag{7}$$

Substituting Eq. (6) in Eq. (7) gives a solution for characteristic length, given by:

$$x_c = \frac{4a^3 k_x \lambda}{3\mu_x F_z} - a \tag{8}$$

Remark 1: Another way to obtain characteristic length x_c is to apply the continuity condition on the stress distribution, i.e. $\lim_{x \rightarrow x_c^+} \sigma(x) = \lim_{x \rightarrow x_c^-} \sigma(x)$

After integration and substitution of characteristic length from Eq. (8), the generated force in tire/ground contact patch would be obtained as [18]:

$$F_x = 2a^2k_x\lambda\left(1 - \frac{\lambda}{\lambda^*}\right)^2 + \mu_x F_z \left(\frac{\lambda}{\lambda^*}\right)^2 \left(3 - 2\frac{\lambda}{\lambda^*}\right) \tag{9}$$

where λ^* is characteristic slip ratio at which sliding begins to occur in entire contact patch length and is determined by applying the equality of stress distribution slopes (see Figure 2) at $x = a$, i.e. $k_x\lambda = \frac{d}{dx}(\mu_x q_z)|_{x=a}$ which leads to,

$$\lambda^* = \frac{3\mu_x F_z}{2a^2k_x} \tag{10}$$

At the characteristic slip ratio, the interacting force reaches its maximum possible, called peak traction force, and the corresponding coefficient of friction is also known as the peak value of the coefficient of friction (in Figure 3). At first glance, it seems that the interacting force should remain constant as the slip ratio increases, but in fact, as the slip ratio increases, the longitudinal coefficient of friction reduces gradually and eventually at $\lambda = 1$ achieves a lower value than the peak value, called sliding coefficient of friction. This phenomenon can be roughly expressed via a linear function. Therefore, the interacting tire/ground force would be given by [8]:

$$F_x = \begin{cases} 2a^2k_x\lambda\left(1 - \frac{\lambda}{\lambda^*}\right)^2 + \mu_p F_z \left(\frac{\lambda}{\lambda^*}\right)^2 \left(3 - 2\frac{\lambda}{\lambda^*}\right) & \lambda \leq \lambda^* \\ F_z \left(\mu_p + \frac{\mu_s - \mu_p}{\lambda^* - 100\%}\right) (\lambda^* - \lambda) & \lambda > \lambda^* \end{cases} \tag{11}$$

Although linear approximation is not accurate to interpret the interacting force in the unstable zone, in this paper, the major concentration is laid on the stable zone, and the influence of linearised assumption in the unstable zone on the results is excluded. In fact, in the stable zone, the generated force is the reaction to driving torque. Accordingly, as driving torque increases from zero, the tire bristle deforms, and consequently a corresponding tractive force is generated in the contact patch. This fact will continue until the tractive force achieves the peak value, namely $\mu_p F_z$, referred to as a stable zone in Figure 3. A further increase of driving torque will produce a larger tire slip and enters the tire in the unstable zone. The reason for the decrease of tractive force in the unstable zone is that the longitudinal coefficient of friction reduces as slip ratio increases. This terminology is chosen since in stable zone increase of driving torque leads to a larger slip ratio and therefore a larger tractive force is generated in contact patch which limits the tire slip. But in the unstable zone, an increase of slip ratio due to a larger driving torque ends in tractive force reduction, which underlies an additional increase of tire slip and so on.

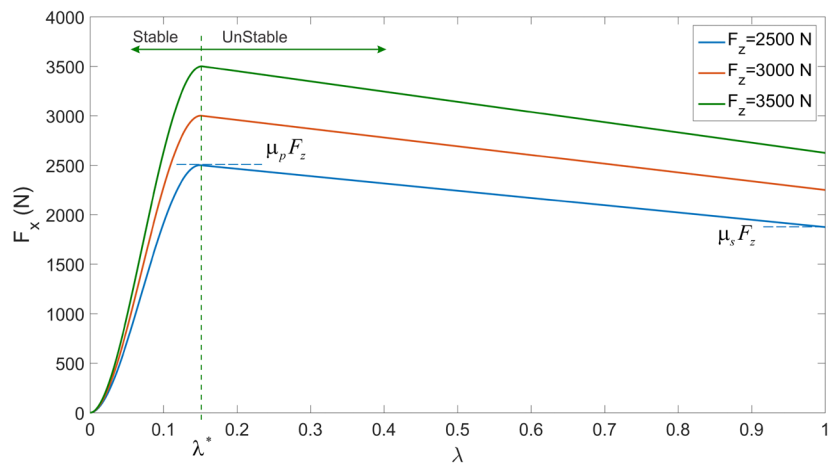


Figure 3. F - λ diagram.

MODIFIED VEHICLE LONGITUDINAL MODEL

A free-body diagram of a front-wheel-drive (FWD) vehicle is shown in Figure 4. To study the dynamics of a rolling and slipping wheel, the drive wheel is shown separately in the figure. Acting forces on vehicle body include air drag (F_D), grade resistance (F_{Gr}), inertia (F_{in}), and rolling resistance of the non-drive wheels ($F_{R,n}$). According to the free-body diagram of the wheel, a driving torque (T_w) is applied through the powertrain system that is opposed by rotational inertia

($I\dot{\omega}$) and rolling resistance torque¹ ($T_{R,d}$). It is notable that for the rolling resistance to be appeared in the vehicle equation of motion together with other resistive forces, usually rolling resistance torque is neglected in the wheel equation of motion [4,5,19–21]. The wheel/body reaction force (F_{WB}) and transitional inertia of the drive wheel is applied to the wheel centre. Considering the equilibrium equations for vehicle body and wheel, Eq. (12) and (13) are obtained, respectively.

$$F_{BW} = F_D + F_{Gr} + F_{in} + F_{R,n} \tag{12}$$

$$T_w - I\dot{\omega}_w = F_x r_{dyn} \tag{13}$$

In the above equations, F_{BW} and F_x are body to wheel interaction force and tractive force, respectively. If a no-slip assumption is made through the driveline, i.e. engine, transmission, and final drive angular speeds are correlated by the gear ratio, then I as the equivalent moment of inertia is given by Eq. (14) [20]:

$$I = (I_e + I_{tr})i_{tr}^2 i_f^2 + I_d i_f^2 + I_w \tag{14}$$

where I_e, I_{tr}, I_d , and I_w are engine, transmission, driveshaft, and wheel moment of inertia, respectively. Also, i_{tr} and i_f are transmission and final drive gear ratios, respectively.

To obtain the vehicle equation of motion, we may use the virtual work principle. By applying virtual angular and translational displacements, namely $\delta\theta$ and δx , to the wheel and vehicle body, respectively, one may obtain:

$$(T_w - I\dot{\omega}_w - T_{R,d})\delta\theta - (F_{WB} + m_w a_x)\delta x - F_x(r_{dyn}\delta\theta - \delta x) = 0 \tag{15}$$

Since the virtual displacements should obey the kinematic constraints of the system, analogous to Figure 1 and Eq. (3), we apply the condition $\delta x = r_{eff}\delta\theta$ to Eq. (15). Hence, for non-zero virtual displacements, Eq. (15) can be rewritten as:

$$T_w - I\dot{\omega}_w - T_{R,d} - (F_{WB} + m_w a_x)r_{eff} - \lambda F_x r_{dyn} = 0 \tag{16}$$

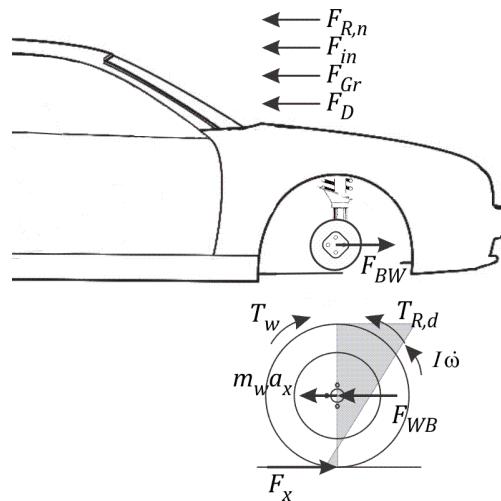


Figure 4. Free body diagrams of vehicle body and wheel.

We already know that wheel and body action/reaction forces, namely F_{BW} and F_{WB} , are equal. In addition, F_{in} in Eq. (12) includes the inertia of the vehicle body and its attachments except for the transitional inertia of the drive wheels, i.e. $m_w a_x$. As a result, by substituting Eq. (12) and Eq. (13) into Eq. (16) and performing some simplifications, the vehicle equation of motion would be described by:

$$m\ddot{x} = F_x - F_D - F_{Gr} - F_{R,n} - \frac{T_{R,d}}{r_{eff}}; 0 \leq \lambda < 1 \tag{17}$$

where m and \ddot{x} are vehicle mass and longitudinal acceleration, respectively. Combining Eq. (3) and Eq. (17) yields:

¹Rolling resistance is originated from asymmetric normal force distribution at contact patch that results in an opposing torque. Usually the equivalent force is considered in longitudinal modeling, while in order to achieve a valid model using virtual work principle, the original torque is considered here.

$$m\ddot{x} = F_x - F_D - F_{Gr} - F_{R,n} - \frac{F_{R,d}}{(1-\lambda)}; 0 \leq \lambda < 1 \tag{18}$$

where $F_{R,d} = \frac{T_{R,d}}{r_{dyn}}$ is defined as the rolling resistant force of the drive wheels.

Neglecting the tire longitudinal slip forms the simplified model, which has been widely used in order to analyse the longitudinal motion of ground vehicles. Nevertheless, this neglect leads to an unbalanced power flow within the powertrain and vehicle (proof given in Appendix 2).

Remark 2: According to Eq. (17) and (18), a numerical divergence is expecting to occur when the wheel comes to a spin, i.e. slip becomes 100%. It should be brought under consideration that the wheel spin usually happens momentarily since as soon as tractive force is being generated in the contact patch, longitudinal acceleration becomes positive, and consequently, its integration, namely longitudinal speed, would be a non-zero positive too. However, to avoid numerical divergence in simulations, a modified slip ratio is recommended for the speeds lower than a threshold v_{th} given by [22]:

$$\lambda = \frac{2v_{th}(r_{dyn}\omega_w - v_x)}{2v_{th}(r_{dyn}\omega_w - v_x) + v_{th}^2 + v_x^2}; v_x < v_{th} \tag{19}$$

Remark 3: In order to utilise Eq. (18) in backward simulations, where vehicle speed and acceleration are assumed to be known a priori, an appropriate inverse tire model should be used in which the tire slip is provided for a specific tractive force under determined conditions. A polynomial inverse tire model is provided by Sina et al. [23], in which the coefficients are characterised as a function of performance parameters. Interested readers may refer to that paper for further details.

RESISTANT POWERS

Figure 5 illustrates a schematic of power flow through the vehicle powertrain. The output power of the internal combustion engine, after subtraction of driveline and tire losses, is consumed to overcome the resistant powers, i.e. aerodynamic drag, road grade, and inertia, which are given by:

$$P_D = F_D v_x = \frac{1}{2} \rho_a c_D A_f v_{rel}^2 v_x \tag{20}$$

$$P_{Gr} = F_{Gr} v_x = m_v g \sin \theta v_x \tag{21}$$

$$P_{in} = F_{in} v_x = (m_v + m_{eq}) a_x v_x \tag{22}$$

Moreover, usually tire loss is also considered as a resistant power in analysing the vehicle longitudinal motion [4,10,11,20,21,24]. Therefore, with regard to the difference between the circumferential speed of the drive and non-drive wheels as a consequence of the tire slip, resistant power due to rolling resistance at non-drive and drive axles can be given by Eq. (23) and Eq. (24), respectively.

$$P_{R,n} = F_{R,n} v_x = f_R F_{z,n} v_x \tag{23}$$

$$P_{R,d} = T_{R,d} \omega_w = f_R F_{z,d} r_{dyn} \omega_w \tag{24}$$

In the above equations, the dynamic axle loads should be used, which are given by:

$$F_{z,dyn,f} = F_{z,st,f} - \frac{m_v h}{L} (g \sin \theta + a_x) \tag{25}$$

$$F_{z,dyn,r} = F_{z,r,st} + \frac{m_v h}{L} (g \sin \theta + a_x) \tag{26}$$

It is notable that small fluctuations occur in dynamic axle load due to road irregularities. However, the appropriate design of the vehicle suspension would minimise these fluctuations [25]. Therefore, this effect is usually neglected in longitudinal motion analysis.

Recent studies have shown that tire power loss is comprised of longitudinal slip as well as rolling resistance. Resistant power due to tire longitudinal slip, introduced and validated in [8], is described as:

$$P_S = F_x \lambda r_{dyn} \omega_w \tag{27}$$

Therefore, in the modified model, resistant powers include aerodynamic drag, road grade, inertia, rolling resistance, and tire slip loss or slip resistance, whereas the last term has been neglected in similar studies, which leads to an unbalanced power flow through the driveline (see Appendix 2). Accordingly, the energy demand would be defined as the integration of the resistant power over time, given by:

$$E = \int_{t_0}^{t_f} P dt \tag{28}$$

where t_0 and t_f are initial and final time determined by the driving cycle or a specific manoeuvre. By substituting each of the resistant powers into Eq. (28), relevant energy demand would be obtained during the defined manoeuvre or driving cycle.

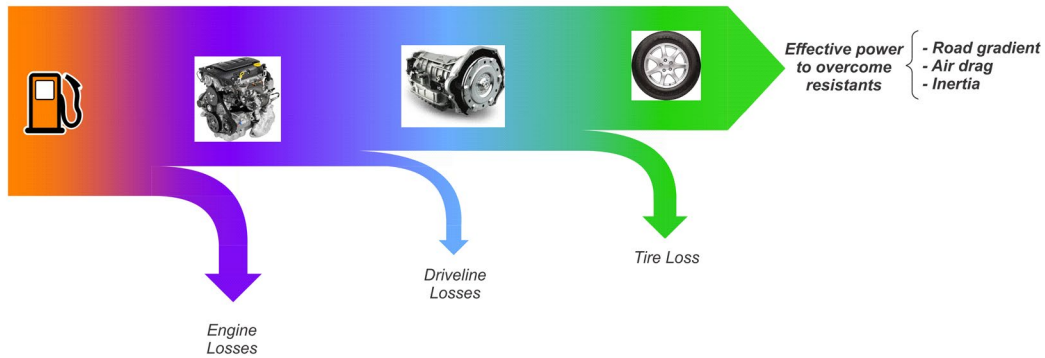


Figure 5. A schematic of the tank to wheel power flow.

RESULTS AND DISCUSSION

Simulations are performed on a B-class sedan with specifications listed in Table 1. In this section, firstly, half-throttle 0 to 100 km/h acceleration is simulated, and after that, vehicle energy demand in some determined driving cycles is discussed.

Table 1. Specifications of the vehicle.

Specification	Description
Vehicle mass	920 kg
Mass distribution (F:R)	57:43
Wheelbase	2345 mm
C.G. height	463 mm
Max. engine power	61 hp @ 5000 rpm
Max. engine torque	103 Nm @ 2800 rpm
No. of gears	5
Gear ratios	3.454:1
	1.944:1
	1.275:1
	0.861:1
	0.692:1
Final drive ratio	3.777:1
Drag coefficient	0.39
Frontal area	1.93 m ²
Rolling resistance coefficient	0.008
Dynamic radius	253 mm
Tire longitudinal stiffness	2300 kN/m ²
Tire vertical stiffness	120 kN/m

Half-Throttle 0-100 km/h Acceleration

Figure 6 illustrates longitudinal acceleration and speed for the half-throttle 0 to 100 km/h acceleration manoeuvre. A 1-second gear shift gap is considered in the simulations. Due to the large tractive force at low gears, especially first gear, a relatively large longitudinal slip occurs, and this makes the modified model more significantly different from the simplified model. However, as the gear is shifted up, the tractive force and tire slip would be reduced, and as a consequence, the difference between simplified and modified models would be diminished. In the simplified model, due to a greater acceleration comparing to the modified model, speed grows faster at the first and second gears, but the

difference remains almost constant as the gear is shifted up. The dimensionless variable λ increases to about 8% at the first gear and then is limited to about 3%, 1.5%, and 1% at the second, third, and fourth gears, respectively. A decreasing trend of slip ratio is expected in higher gears, if available, which leads to less difference between the response of modified and simplified models.

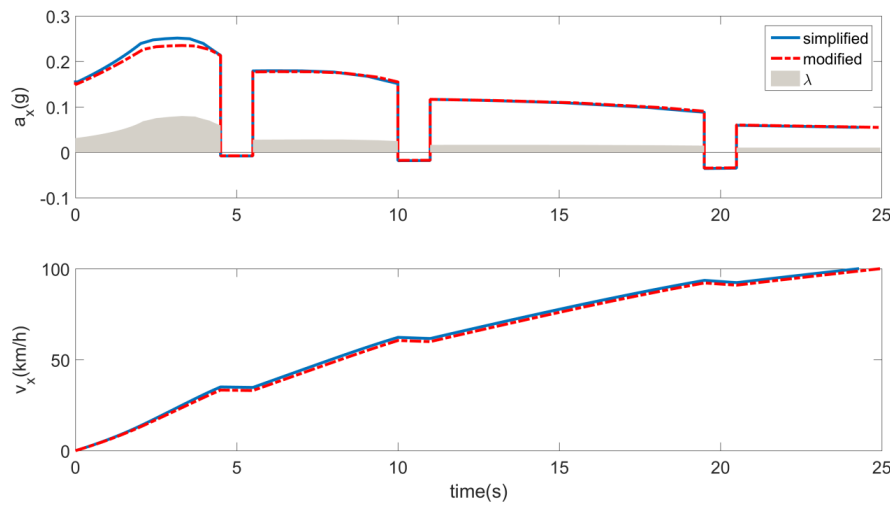


Figure 6. Comparing longitudinal acceleration and speed for the simplified and modified models.

A comprehensive illustration of energy breakdown at each engaged gear is shown in Figure 7. At the first gear, the consumed energy in the modified model is increased by 12.2%, and the slip loss share is much higher than the rolling resistance and aerodynamic drag. Thus, slip loss neglect leads to a notable error in energy demand analysis. However, slip loss becomes insignificant at the third and fourth gears, and tire loss is highly determined by the rolling resistance rather than slip resistance. Consequently, tire slip loss is of minor importance, and its omission does not obviously affect the results. According to Figure 7, the difference between the simplified and modified model in the third and fourth gears is less than 2%. Additionally, tire slip loss becomes entirely negligible comparing to other sources of resistance, i.e. inertia, aerodynamic drag, and rolling resistance.

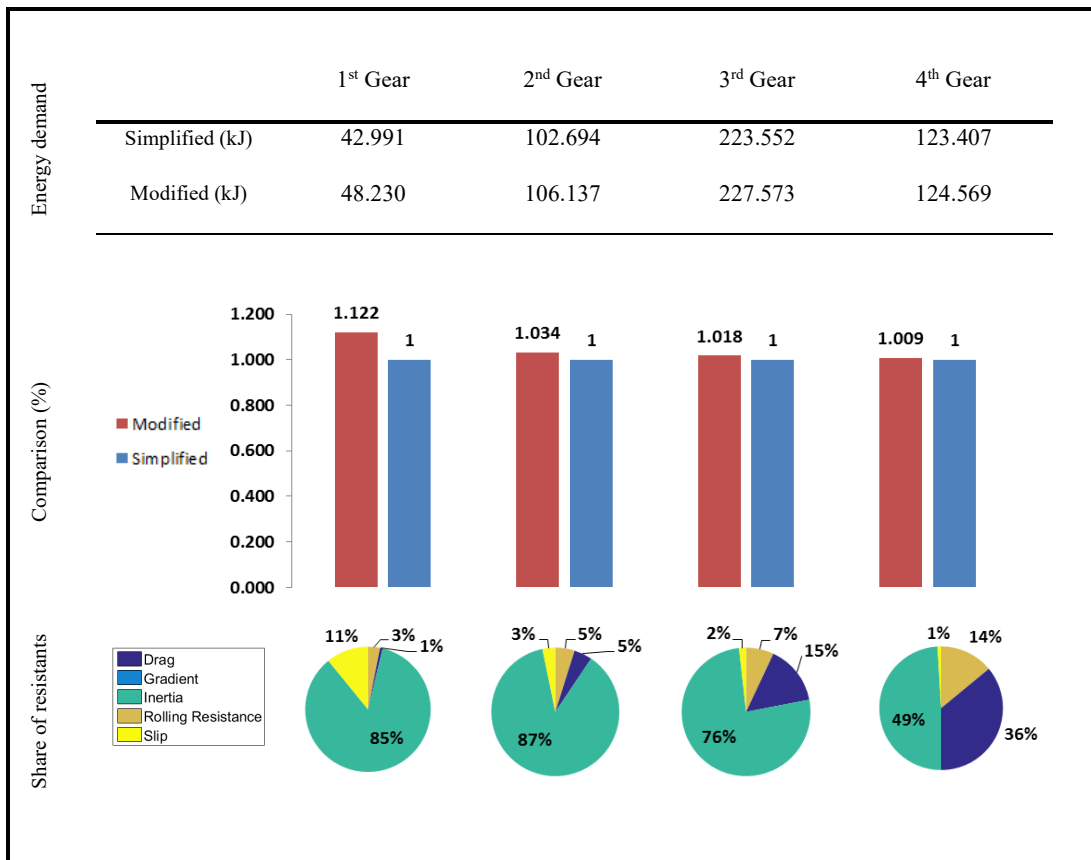


Figure 7. A comprehensive comparison between simplified and modified models in each gear.

Figure 8 shows the energy demand and share of each resistance for the whole manoeuvre. The energy demand of the simplified model is less due to neglecting the tire slip loss, which includes 2.5% of the total consumed energy. As expected, inertia loss in this manoeuvre is dominant, including about 75% of the total losses. The consumed energy due to modified tire resistance, including rolling and slip losses, has been significantly increased in comparison to that of due to simplified or rolling resistance. Table 2 summarises the increase of consumed energy in tires considering the modified tire loss comparing to rolling resistance. At the first gear, the consumed energy due to tire slip, i.e. 5.2 kJ, is three and a half times greater than the consumed energy due to rolling resistance. However, slip loss decreases gradually as the tractive force drops at higher gears, but even at the fourth gear, the modified model improves the prediction accuracy of the tire loss by 6.7%. In the whole manoeuvre, considering the modified tire resistance increases the consumed energy of tires by about 35%. Hence, considering the modified tire loss could considerably increase the accuracy of tire resistance prediction.

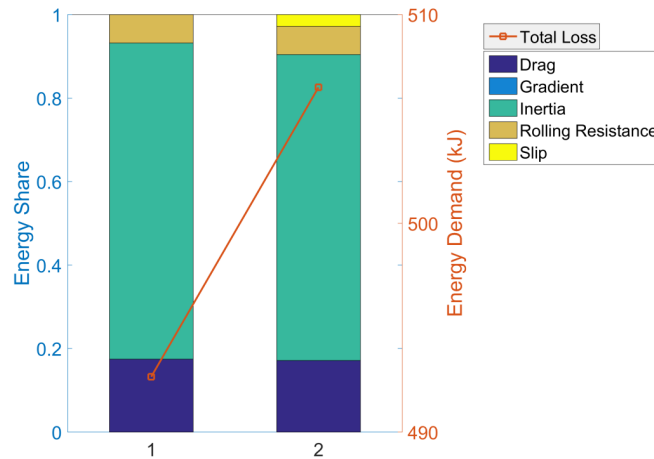


Figure 8. Energy demand and share of each resistance in the 0-100 km/h acceleration manoeuvre (with 1: simplified model, 2: modified model).

Table 2. Consumed energy due to rolling resistance and slip loss.

	1 st gear	2 nd gear	3 rd gear	4 th gear	Overall
Consumed energy due to rolling resistance (kJ)	1.490	5.177	15.852	17.471	39.990
Consumed energy due to slip loss (kJ)	5.239	3.443	4.021	1.162	13.865
Increase of modified tire loss w.r.t rolling resistance (%)	351.6	66.5	25.4	6.7	34.7

The manoeuvre selected to establish the results is not a severe manoeuvre and is likely to be repeated in everyday driving. The database used to develop worldwide harmonised light vehicles test procedure (WLTP) cycle implies that many drivers accelerate by about 2.77 m/s² in the US and by about 2.22 m/s² in the EU and Japan [26], which is close to the maximum acceleration obtained in the simulations, 2.30 m/s² or 0.23g. In a more aggressive driving condition, the difference between simplified and the modified longitudinal model would be increased, and the tire slip loss becomes larger due to a higher tire slip.

Driving Cycles

Three driving cycles, i.e. WLTP, new European driving cycle (NEDC), and Federal test procedure (FTP), are selected to compare the energy demand using the modified and simplified vehicle models. Table 3 compares some important attributes of the selected driving cycles. NEDC has gentler positive and negative acceleration in comparison to WLTP and FTP driving cycles. It comprises four repeated ECE-15 urban driving cycles, corresponds to 0 to 780 seconds, and an extra-urban driving cycle (EUDC) that starts from 780th second and lasts to the end of the cycle, namely 1180th second. However, owing to the CO₂ emissions gap between real-world and type approvals based on NEDC [27], the WLTP cycle has been developed. Since WLTP is extracted from in-use driving data, it provides more consistency with real-world fuel consumption and emissions [10,28]. This driving cycle has higher positive and negative accelerations as well as increased maximum and average speeds. Thus, it can be inferred that WLTP is more aggressive. FTP driving cycle is defined by the Environmental Protection Agency (EPA) and represents city driving conditions with frequent stops and moderately high accelerations.

Vehicle energy demand and share of each resistance in the selected driving cycles is shown in Figure 9 for the simplified and modified vehicle models. Energy demand per kilometre in NEDC and FTP cycles are almost close to each other, while in WLTP, as a result of its aggressiveness, energy demand has been increased significantly. Owing to the WLTP introduction, which is going to be used in vehicles' type approval tests, an increase of energy demand should be prefigured in the design and development of powertrains to meet CO₂ targets. Simulation results are summarised in

Table 4. As it can be observed, the largest share of energy demand in the FTP cycle belongs to inertia and in WLTP and NEDC cycles belongs to aerodynamic drag. In addition, the share of rolling resistance loss is decreased in WLTP in comparison to the NEDC cycle, whereas the share of aerodynamic drag and inertia face a slight increase. Energy loss due to tire slip is highly determined by the tractive force, and therefore in WLTP, which represents a more aggressive cycle, it has the largest value, while in the NEDC cycle, the least amount is achieved.

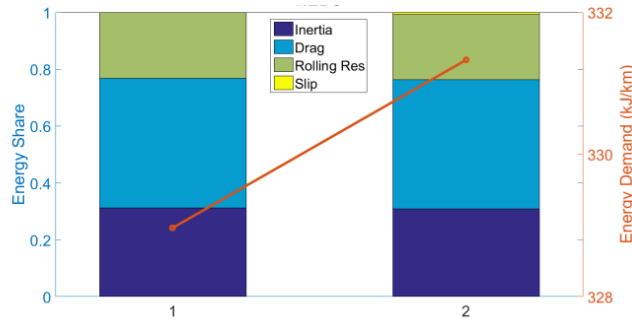
Table 3. Specifications of the selected driving cycles [29,30].

Parameter	NEDC	WLTP	FTP
Total time (s)	1180	1800	1874
Standing time (s)	241	235	335
Total distance (m)	10932	23266	17770
Percentage of time standing	20.4	13.4	17.9
Max. speed (km/h)	120	131	91
Average driving speed (km/h)	43.1	53.5	39.2
Average speed (km/h)	33.3	46.5	34.2
Max. negative acceleration (m/s ²)	-1.39	-1.5	-1.47
Max. positive acceleration (m/s ²)	1.06	1.666	1.475

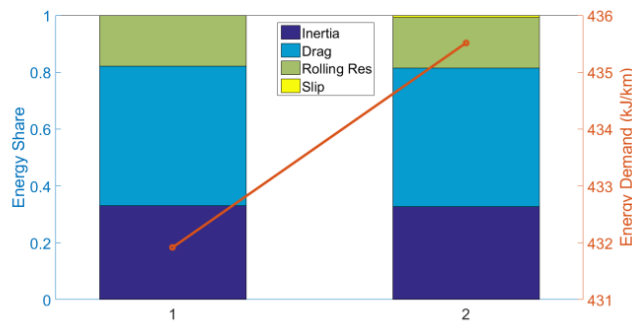
Table 4. Summary of energy demand analysis.

Parameter	NEDC	WLTP	FTP
Energy demand using modified model (kJ/km)	331.3	435.5	344.8
Energy demand difference between simplified and modified models (%)	0.7	0.8	0.9
Share of inertia (%)	30.9	32.7	46.4
Share of aerodynamic drag (%)	45.4	48.8	30.8
Share of rolling resistance (%)	23.0	17.7	22.0
Simplified tire resistance (kJ/km)	76.3	77.1	75.7
Modified tire resistance (kJ/km)	78.7	80.7	78.7
Difference between simplified and modified tire resistance (%)	3.1	4.7	4.0

Tire slip comprises about 1 % of the total consumed energy in each of the driving cycles, which seems to be negligible at first glance, but taking this assumption into account would enhance the accuracy of tire resistance prediction by 3-5%. Additionally, in a more aggressive driving cycle, tire slip loss would experience a considerable increase so that its amount in NEDC (2.4 kJ/km) has been increased by 25% and 50% in FTP and WLTP cycles respectively, and further increments are expected in real-world driving.



(a) NEDC



(b) WLTP

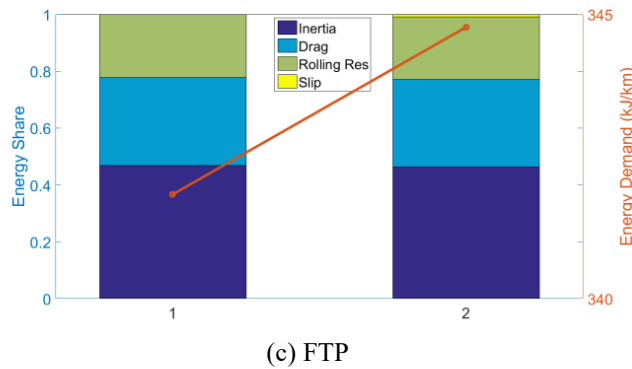


Figure 9. Energy demand and share of each resistance in the selected driving cycles (with 1: simplified model, 2: modified model).

CONCLUSION

A modified dynamic model for longitudinal motion of the ground vehicles is proposed. In the modified model, the actual motion of the drive wheels, i.e. rolling with slip, is considered to extract the equation of motion, which makes the proposed model more compliant with the physical nature of the tire and vehicle motion. The modified model provides a notable difference in comparison to the simplified model provided that the tractive force is large enough. In 0 to 100 km/h acceleration manoeuvre, tire slip is significant at low gears, and this makes the modified model more notably different from the simplified model. In such a case, the consumed energy due to tire slip is considerable and neglecting that the energy breakdown analysis highly affects the validity of the analysis. Furthermore, a significant improvement in the accuracy of tire resistance prediction could be observed under the light of employing the modified model.

ACKNOWLEDGEMENT

The authors acknowledge the contributions of Dr Ali Salavati-Zadeh.

REFERENCES

- [1] Sarhadi P, Yousefpour S. State of the art: hardware in the loop modeling and simulation with its applications in design, development and implementation of system and control software. *International Journal of Dynamics and Control* 2015;3:470–479.
- [2] Ahmad F, Mazlan SA, Zamzuri H, et al. modelling and validation of the vehicle longitudinal model. *International Journal of Automotive and Mechanical Engineering* 2014;10:2042–2056.
- [3] Alexander A, Vacca A. Longitudinal vehicle dynamics model for construction machines with experimental validation. *International Journal of Automotive and Mechanical Engineering* 2017;14(4):4616–4633..
- [4] Wong JY. *Theory of ground vehicles*. 3rd ed. New York: John Wiley and sons; 2001.
- [5] Marzbanrad J, Tahbaz-zadeh Moghaddam I. Self-tuning control algorithm design for vehicle adaptive cruise control system through real-time estimation of vehicle parameters and road grade. *Vehicle System Dynamics* 2016;54:1291–1316.
- [6] Hashemi E, Kasaiezadeh A, Khosravani S, Khajepour A, Moshchuk N, Chen S-K. Estimation of longitudinal speed robust to road conditions for ground vehicles. *Vehicle System Dynamics* 2016;54:1120–1146.
- [7] IEA. *Energy technology perspectives*. Report, IEA, Paris, May 2015.
- [8] Sina N, Esfahanian V, Hairi Yazdi MR, Azadi S. Introducing the modified tire power loss and resistant force regarding longitudinal slip. *SAE International Journal of Passenger Cars—Mechanical Systems* 2018;11:06-11-02–0014.
- [9] Sina N, Nasiri S, Karkhaneh V. Effects of resistive loads and tire inflation pressure on tire power losses and CO₂ emissions in real-world conditions. *Applied Energy* 2015;157:974–983.
- [10] Pavlovic J, Marotta A, Ciuffo B. CO₂ emissions and energy demands of vehicles tested under the NEDC and the new WLTP type approval test procedures. *Applied Energy* 2016;177:661–670.
- [11] Pavlovic J, Ciuffo B, Fontaras G, et al. How much difference in type-approval CO₂ emissions from passenger cars in Europe can be expected from changing to the new test procedure (NEDC vs. WLTP)? *Transportation Research: Part A Policy Pract* 2018;111:136–47.
- [12] d’Ambrosio S, Vitolo R. Potential impact of active tire pressure management on fuel consumption reduction in passenger vehicles. *Proceedings of the Institution of Mechanical Engineers, Part D Journal of Automobile Engineering* 2019;233(4):961–975.
- [13] d’Ambrosio S, Vitolo R, Salamone N, Oliva E. Active tire pressure control (ATPC) for passenger cars: design, performance, and analysis of the potential fuel economy improvement. *SAE International Journal of Passenger Cars - Mechanical Systems* 2018;11:2018-01–1340.
- [14] ISO 8855:2011. *Road vehicles- vehicles dynamics and road-holding ability- vocabulary*.
- [15] SAE J670_197607:1976. *Vehicle dynamics terminology*.

- [16] Li J, Zhang Y, Yi J. A hybrid physical-dynamic tire/road friction model. *Journal of Dynamic Systems, Measurement, and Control* 2012;135:011007.
- [17] Pacejka HB. *Tire and vehicle dynamics*. 3rd ed. Oxford: Butterworth-Heinemann; 2002.
- [18] Svendenius J. *Tire modeling and friction estimation*. Lund: Lund University; 2007.
- [19] Rajamani R. *Vehicle dynamics and control*. 2nd ed. New York: Springer; 2012.
- [20] Gillespie TD. *Fundamentals of vehicle dynamics*. Warrendale, PA: SAE International; 1992.
- [21] Onori S, Serrao L, Rizzoni G. *Hybrid electric vehicles*. London: Springer London; 2016.
- [22] Mathworks. *MATLAB user's guide*. 2015.
- [23] Sina N, Hairi Yazdi MR, Esfahanian V. A novel method to improve vehicle energy efficiency: Minimisation of tire power loss. *Proceeding of Institution of Mechanical Engineers, Part D Journal of Automobile Engineering* 2020;234:1153–1166.
- [24] Qiu S, Qiu L, Qian L, Pisu P. Hierarchical energy management control strategies for connected hybrid electric vehicles considering efficiencies feedback. *Simulation Modelling Practice and Theory* 2019;90:1–15.
- [25] Nasiri S, Sina N, Eslami A. Multi-objective optimisation of McPherson strut suspension mechanism kinematics using random search method. *Indian Journal of Science and Technology* 2015;8(16):1-10.
- [26] Tutuianu M, Bonnel P, Ciuffo B, et al. development of the worldwide harmonised light duty test cycle (WLTC) and a possible pathway for its introduction in the European legislation. *Transportation Research Part D: Transport and Environment* 2015;40:61–75.
- [27] Martin NPD, Bishop JDK, Choudhary R, Boies AM. Can UK passenger vehicles be designed to meet 2020 emissions targets? A novel methodology to forecast fuel consumption with uncertainty analysis. *Applied Energy* 2015;157:929–939.
- [28] Andersson J, May J, Favre C, et al. On-Road and Chassis dynamometer evaluations of emissions from two euro 6 diesel vehicles. *SAE International Journal of Fuels and Lubricants* 2014;7:2014-01–2826.
- [29] Barlow TJ, Latham S, McCare IS, Boulter PG. *A reference book of driving cycles for use in the measurement of road vehicle emissions*. Wokingham: Transport Research Laboratory; 2009.
- [30] Giakoumis EG. *Driving and Engine Cycles*. Cham: Springer International Publishing; 2017.

APPENDIX 1

Consider a strip, perpendicular to the plane, located at any arbitrary point in the adhesion region. Within a short time interval Δt , the strip deformation is the difference between the distance that strip travels due to circumferential and linear velocity, given by Eq. (A-1).

$$\delta = (r_{dyn}\omega_w - v_x)\Delta t \tag{A-1}$$

In addition, the location of strip is defined by:

$$x(t) = r_{dyn}\omega_w\Delta t \tag{A-2}$$

Tire deformation can be defined as a function of slip ratio λ , by combining the two above equations:

$$\delta(x) = \frac{(r_{dyn}\omega_w - v_x)}{r_{dyn}\omega_w}x = \lambda x \tag{A-3}$$

APPENDIX 2

Power balance equation within the vehicle and powertrain must be always satisfied, i.e. the generated power must be equal to power losses, including those lost through the driveline and those arise out of resistive loads (i.e. grade resistant, air drag, and inertia). Therefore, power balance equation could be given by:

$$P_e = \sum P_{driveline} + \sum P_{res} \tag{A-4}$$

By definition, power is the multiplication of torque and angular velocity. The generated power in engine (or other propulsion systems, e.g. electric motors) is given by Eq. (A-5).

$$P_e = T_e\omega_e \tag{A-5}$$

Analogously, the power transmitted to the drive wheels can be given by:

$$P_w = T_w\omega_w = \eta T_e\omega_e \tag{A-6}$$

where η represents the driveline efficiency. The difference between engine output power and transmitted power to the wheel is the lost power through the driveline that equals to $(1 - \eta)P_e$. Thus, Eq. (A-4) can be rewritten as:

$$P_e = (1 - \eta)P_e + \sum P_{res} \tag{A-7}$$

Combining Eq. (A-6) and (A-7) yields:

$$P_w = \sum P_{res} \tag{A-8}$$

By substituting the resistant powers from Eq. (20) to Eq. (25) in Eq. (A-8), we obtain:

$$P_w = (F_{in} + F_D + F_{Gr} + F_{R,n})v_x + T_{R,d}\omega_w + F_x\lambda r_{dyn}\omega_w \tag{A-9}$$

For the sake of simplicity, we neglect the rotational inertia of driveline in this part. Hence, the drive torque applied to the wheel according to Figure 4 and Eq. (13) is given by:

$$T_w = F_x r_{dyn} \tag{A-10}$$

Substituting Eq. (A-10) into Eq. (A-6) and then into left-hand side of Eq. (A-9) results in:

$$F_x r_{dyn}\omega_w = (m\ddot{x} + F_D + F_{Gr} + F_{R,n})v_x + T_{R,d}\omega_w + F_x\lambda r_{dyn}\omega_w \tag{A-11}$$

After some simplifications and by recalling Eq. (2), Eq. (A-11) may be rewritten as:

$$F_x v_x = (m\ddot{x} + F_D + F_{Gr} + F_{R,n})v_x + F_{R,d}r_{dyn}\omega_w \tag{A-12}$$

The tractive force in the modified model is given by:

$$F_x = m\ddot{x} + F_D + F_{Gr} + F_{R,n} + \frac{F_{R,d}}{(1 - \lambda)} \tag{A-13}$$

Replacing the tractive force given by Eq. (A-13) in left-hand side of Eq. (A-12) yields:

$$\left(m\ddot{x} + F_D + F_{Gr} + F_{R,n} + \frac{F_{R,d}}{1 - \lambda}\right)v_x = (m\ddot{x} + F_D + F_{Gr} + F_{R,n})v_x + F_{R,d}r_{dyn}\omega_w \tag{A-14}$$

which is equal to right-hand side of Eq. (A-12). Thus, the modified model satisfies the power balance through the driveline. Nevertheless, if tire slip is neglected in the vehicle longitudinal model, there will exist an unbalance term in power balance equation that is equal to $F_{R,d}\lambda r_{dyn}\omega_w$.